

A Fast Wheel-Rail Forces Calculation Computer Code

OLDRICH POLACH
ADtranz, Winterthur, Switzerland

SUMMARY

In the simulations of rail vehicle dynamic behaviour, the computation of wheel-rail forces is repeated many times. Therefore a short calculation time is very important. A fast algorithm and computer code for the computation of wheel-rail forces under known contact geometry and creep and spin conditions is presented in the paper. The proposed method assumes ellipsoidal contact area and normal stress distribution according to Hertz. Because of the short calculation time it can be used instead of simple formulas to improve the accuracy or as a substitution of Kalker's programme FASTSIM to save the computation time. The method has been tested and used in different simulation tools with very good experience. The computer code and some test results given in the appendix allow to apply this method in the user's own computer simulation programmes.

1. INTRODUCTION

The calculation of wheel-rail contact forces has always been important because of analysis of dynamic behaviour of rail vehicles, their running qualities and forces and stresses acting on the track. In a computer simulation, the computation of wheel-rail forces is repeated many times. Therefore a short calculation time is very important.

The exact theory by Kalker (computer programme CONTACT [1]) is not possible to use in the simulations because of its very long calculation time. The simplified theory used in Kalker's programme FASTSIM [2] is much faster than the exact theory, but the calculation time is also often too long for use in complicated multi-body systems.

Searching for faster methods some authors found approximations with simple saturation functions (e.g. [4]). The calculation time using these approximations is short, but there are significant differences to the exact theory.

Another possibility for computer simulations consists in the use of look-up tables with saved pre-calculated values. Because of the limited data in the look-up table, there are differences to the exact theory as well. Large tables are more exact, but the searching in such large tables consumes calculation time.

Disadvantages mentioned above can be avoided by using the proposed algorithm. In spite of the simplifications used, spin is considered. Because of the short calculation time, the creation of a look-up table is not necessary. In comparison to other approximation methods, a smaller difference between the calculated values and the exact theory can be achieved.

The paper contains the theoretical background of the algorithm, the computer code

in FORTRAN and some test results to facilitate an application in your own computer simulation programmes.

2. THEORETICAL BACKGROUND

The proposed method assumes the ellipsoidal contact area with semiaxis a , b and normal stress distribution according to Hertz. The maximum value of tangential stress τ at any arbitrary point is

$$\tau_{\max} = f \cdot \sigma \quad (1)$$

where f - coefficient of friction,
 σ - normal stress.

The coefficient of friction f is assumed constant in the whole contact area.

The solution assumes a linear growth of the relative displacement between the bodies from the leading point (A) to the trailing point (C) on the edge of the contact area (Fig. 1). At first the contact surfaces of the bodies stick firmly together and the displacement of the bodies is the result of material creepage (area of adhesion). The tangential stress τ acts against the creep and its value grows linearly with the distance from the leading edge (the assumption is identical with Kalker's simplified theory). If τ in the adhesion area reaches its maximum value according to (1) a relative motion of the contact surfaces appears. This part of contact area is called the area of slip. The tangential stress acts against the slip according to (1).

The tangential force is determined as

$$F = \iint_{(U)} \tau \, dx \, dy \quad (2)$$

where U - contact area.

For vectors in x and y directions we get

$$F_i = F \frac{s_i}{s} \quad i = x, y \quad (3)$$

where

$$s = \sqrt{s_x^2 + s_y^2} \quad (4)$$

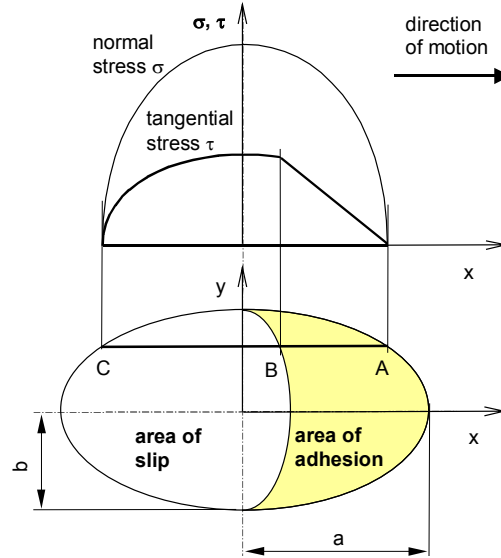


Fig. 1. Assumption of distribution of normal and tangential stresses in the wheel-rail contact area

s_x, s_y - slip in x and y directions

Freibauer [5] has solved the creep-force law without spin using a transformation of the tangential stress distribution ellipsoid to a hemisphere with the formulae

$$y^* = \frac{a}{b} y, \quad \tau^* = \frac{a}{\tau_0} \tau \quad (5)$$

where y^*, τ^* - transformed variables y, τ

τ_0 - the maximum stress in the centre of the contact area

The tangential stress is proportional to slip s and the distance from the leading edge (Fig. 1) with proportionality constant C , which is a value characterising the contact elasticity of the bodies (tangential contact stiffness). The gradient of tangential stress in the area of adhesion is

$$\varepsilon = \frac{2}{3} \frac{C \cdot \pi \cdot a^2 \cdot b}{Q \cdot f} s \quad (6)$$

where Q - wheel load

The tangential force is then

$$F = \tau_0 \frac{b}{a^2} \iint_{(U)} \tau^* dx dy^* = -\tau_0 \frac{b}{a^2} \frac{4}{3} a^3 \left(\frac{\varepsilon}{1 + \varepsilon^2} + \arctan \varepsilon \right) \quad (7)$$

According to the theory of Hertz

$$\tau_0 = \sigma_0 \cdot f = \frac{3}{2} \frac{Q \cdot f}{\pi \cdot a \cdot b} \quad (8)$$

where σ_0 - maximal normal stress in the contact area.

After substitution into (7) we obtain

$$F = -\frac{2 \cdot Q \cdot f}{\pi} \left(\frac{\varepsilon}{1 + \varepsilon^2} + \arctan \varepsilon \right) \quad (9)$$

The vector forces F_x, F_y are calculated from (9) using formulae (3).

When solving the wheel-rail contact problem, the spin is of a considerable importance. Spin is a rotation about the vertical axis z caused by wheel conicity. Further under the title spin we will understand the relative spin ψ which means the angular velocity about z -axis divided by speed v . The spin is

$$\psi = \frac{\omega \cdot \sin \gamma}{v} = \frac{\sin \gamma}{r} \quad (10)$$

where ω - angular velocity of wheel rolling

γ - angle of contact surfaces

r - wheel radius

In the following part a force effect of the spin will be mentioned. The moment effect of spin as well as the moment effect caused by lateral slip are neglected because they are too small in comparison with other moments acting on the vehicle.

At a pure spin the vector force F_x is zero. The centre of rotation is situated on the longitudinal axis of the contact area, but its position depends on the equilibrium of

the forces and is unknown at the beginning of the solution. If the longitudinal semiaxis is too small ($a \rightarrow 0$), the centre of spin rotation is approaching the origin of the co-ordinate system. Using the transformation of the tangential stress distribution ellipsoid to a hemisphere, the lateral tangential force caused by pure spin was found as

$$F_y = \tau_0 \frac{b}{a^2} \iint_{(U)} \tau_y^* dx dy^* = -\frac{3}{8} \pi \cdot \tau_0 \cdot a \cdot b \left[|\varepsilon| \left(\frac{\delta^3}{3} - \frac{\delta^2}{2} + \frac{1}{6} \right) - \frac{1}{3} \sqrt{(1-\delta^2)^3} \right] \quad (11)$$

Using the formula (8) we get

$$F_y = -\frac{9}{16} Q \cdot f \cdot K_M \quad (12)$$

where K_M is

$$K_M = |\varepsilon| \left(\frac{\delta^3}{3} - \frac{\delta^2}{2} + \frac{1}{6} \right) - \frac{1}{3} \sqrt{(1-\delta^2)^3} \quad (13)$$

and δ is

$$\delta = \frac{\varepsilon^2 - 1}{\varepsilon^2 + 1} \quad (14)$$

and creep s in equation (6) is given as $\psi \times a$. However this solution is valid only for $a \rightarrow 0$.

The detailed solution for different relations a/b given by Kalker [3] showed that with an increasing relation a/b the force effect of the spin grows. Looking for a fast solution to be used in simulations, a correction of dependence (11) for $a > 0$ was found. The forces caused by longitudinal and lateral creepages and the lateral force caused by spin are calculated separately. In the equations (3), (4) and (6) instead of the slip s there is resulting slip s_C

$$s_C = \sqrt{s_x^2 + s_y^2} \quad (15)$$

where s_{yC} is given as

$$\begin{aligned} s_{yC} &= s_y + \psi \cdot a & \text{for} & \quad |s_y + \psi \cdot a| > |s_y| \\ s_{yC} &= s_y & \text{for} & \quad |s_y + \psi \cdot a| \leq |s_y| \end{aligned} \quad (16)$$

The resulting force effect in lateral direction is given as the sum of both above described effects respecting the creep saturation as follows

$$F_{yC} = F_y + F_{yS} \quad (17)$$

where F_{yS} - increase of the tangential force caused by the spin.
Its value is

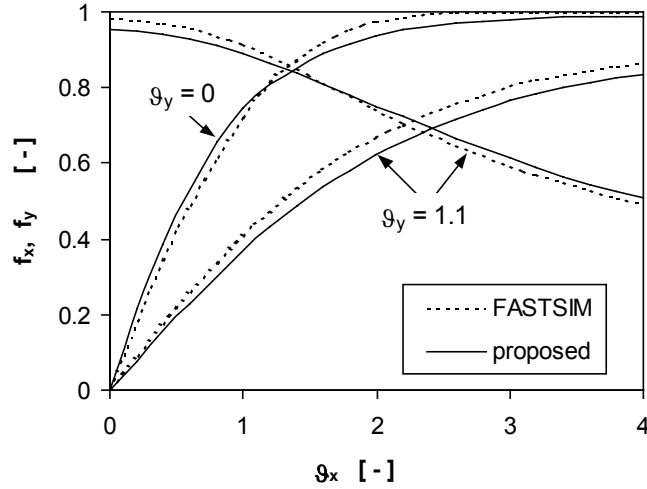


Fig. 2. Comparison of non-dimensional tangential forces caused by longitudinal and lateral creepages

$$F_{yS} = -\frac{9}{16} a \cdot Q \cdot f \cdot K_M \left[1 + 6.3 \left(1 - e^{-\frac{a}{b}} \right) \right] \frac{\psi}{s_C} \quad (18)$$

where K_M is obtained by (13) and ε is actually given as

$$\varepsilon_S = \frac{2}{3} \frac{C \cdot \pi \cdot a^2 \cdot b}{Q \cdot f} \frac{s_{yC}}{1 + 6.3 \left(1 - e^{-\frac{a}{b}} \right)} \quad (19)$$

The contact stiffness C in (6) and (19) can be found by experiments or can be obtained from Kalker's constants [3].

3. USE OF THE PROPOSED METHOD WITH THE CONSTANTS FROM KALKER

The value of the tangential contact stiffness C is derived by assuming an identical linear part of the creep-force law according to Kalker theory and proposed method. According to the proposed theory, if the creep is close to 0 ($\varepsilon \rightarrow 0$), without spin

$$F = -\frac{8}{3} a^2 \cdot b \cdot C \cdot s \quad (20)$$

and according to Kalker

$$F = -G \cdot a \cdot b \cdot c_{jj} \cdot s \quad (21)$$

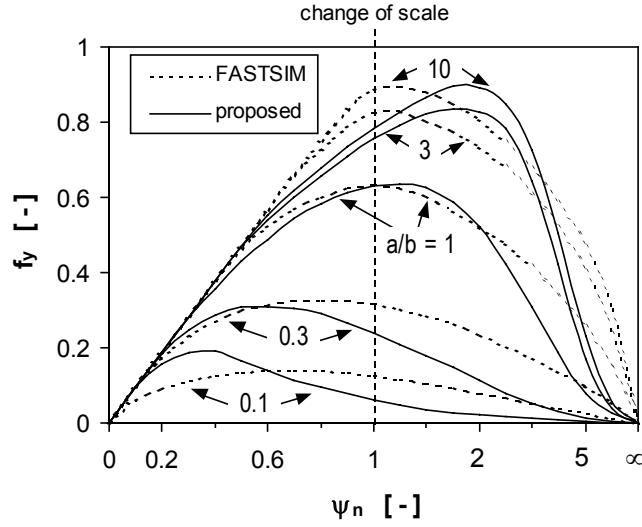


Fig. 3. Comparison of non-dimensional lateral forces caused by pure spin

where c_{jj} – Kalker's constants (c_{11} for longitudinal direction, c_{22} for lateral direction)

After the comparison of (20) with (21) we get

$$C = \frac{3}{8} \frac{G}{a} c_{jj} \quad (22)$$

After the substitution of (22) in (6) the gradient ε of tangential stress is

$$\varepsilon = \frac{1}{4} \frac{G \cdot \pi \cdot a \cdot b \cdot c_{jj}}{Q \cdot f} s \quad (23)$$

Because $c_{11} \neq c_{22}$, constant c_{jj} will be obtained as follows

$$c_{jj} = \sqrt{\left(c_{11} \frac{s_x}{s} \right)^2 + \left(c_{22} \frac{s_y}{s} \right)^2} \quad (24)$$

The lateral force caused by the spin (12) is for $\varepsilon \rightarrow 0$ according to the proposed theory

$$F_y = -\frac{1}{4} \pi \cdot a^3 \cdot b \cdot C_s \cdot \psi \quad (25)$$

and according to Kalker's theory

$$F_y = -G \cdot c_{23} \cdot \psi \cdot \sqrt{(a \cdot b)^3} \quad (26)$$

With comparison of (25) and (26) we get

$$C_s = \frac{4}{\pi} \frac{G \cdot \sqrt{b}}{\sqrt{a^3}} c_{23} \quad (27)$$

After the substitution of (27) in (19) the gradient of tangential stress ε_s used for calculation of spin influence is

$$\varepsilon_s = \frac{8}{3} \frac{G \cdot b \cdot \sqrt{a \cdot b}}{Q \cdot f} \frac{c_{23} \cdot s_{yc}}{1 + 6.3 \left(1 - e^{-\frac{a}{b}} \right)} \quad (28)$$

The comparison of the proposed method with Kalker's programme FASTSIM has been done in the non-dimensional co-ordinates

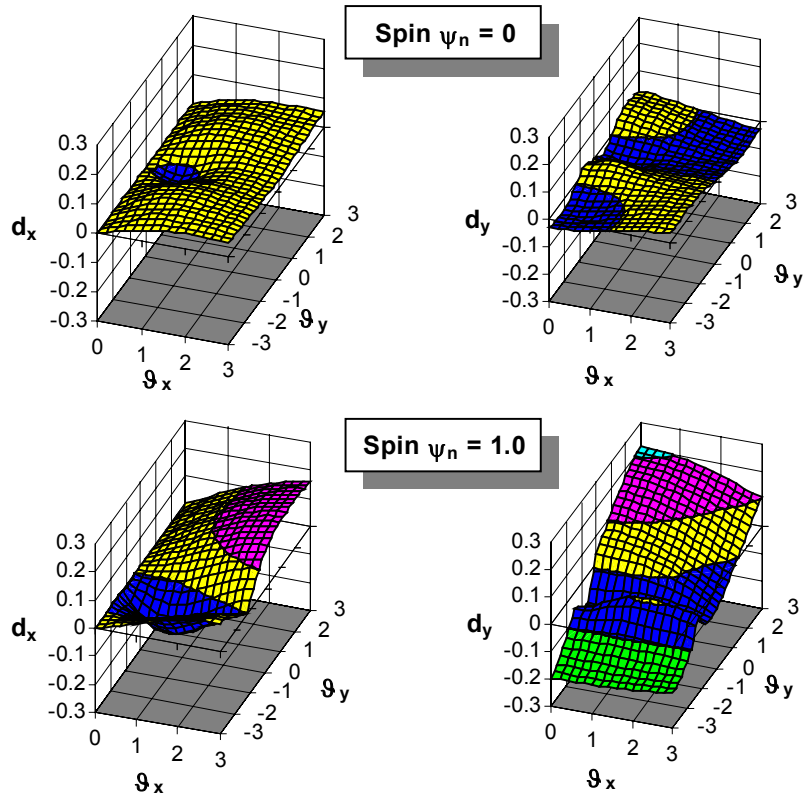


Fig. 4. The difference between the two methods of calculation of the non-dimensional longitudinal (left) and lateral (right) forces in function of creep and spin

- non-dimensional wheel-rail forces

$$f_i = \frac{F_i}{Q \cdot f} \quad i = x, y \quad (29)$$

- non-dimensional creep

$$g_i = \frac{G \cdot a \cdot b \cdot c_{jj} \cdot s_i}{Q \cdot f} \quad i = x, y; \quad j = 1 \text{ for } i = x, j = 2 \text{ for } i = y \quad (30)$$

- non-dimensional spin

$$\psi_n = \frac{G \cdot (\sqrt{a \cdot b})^3 \cdot c_{23} \cdot \psi}{Q \cdot f} \quad (31)$$

The results of the tangential forces caused by longitudinal and lateral creepages are shown in Fig. 2, the comparison of lateral forces caused by pure spin is given in Fig. 3. Fig. 4 shows the difference of longitudinal and lateral non-dimensional forces under different creep and spin conditions computed with the proposed method and with the programme FASTSIM. The difference was defined as follows

$$d_i = f_{iK} - f_{iP} \quad i = x, y \quad (32)$$

where f_{iK} – non-dimensional force computed with FASTSIM ($n=30$, where n is number of slices in FASTSIM)

f_{iP} – non-dimensional force computed with the proposed method

The greatest, though very rarely occurring differences amount to less than 0.3, which is acceptable for practical use in railway vehicle dynamics. However the proposed algorithm is about 17 times faster than the programme FASTSIM with recommended number of slices $n=10$ (Fig. 5). The computation time profit using this method in the simulations of rail vehicle dynamics depends, of course, on the structure of the tools. Tests in different programmes give a 3 to 8 times faster calculation time as compared to FASTSIM.

The computer code for use of proposed method as a fast approximation of Kalker's solution can be found in the appendix. There are also some examples which allow to control the results and to apply this method in the user's own computer simulation programmes.

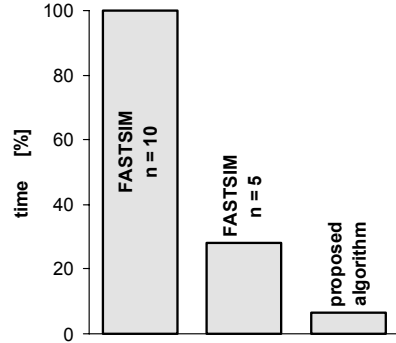


Fig. 5. Comparison of calculation time (n – number of slices in FASTSIM)

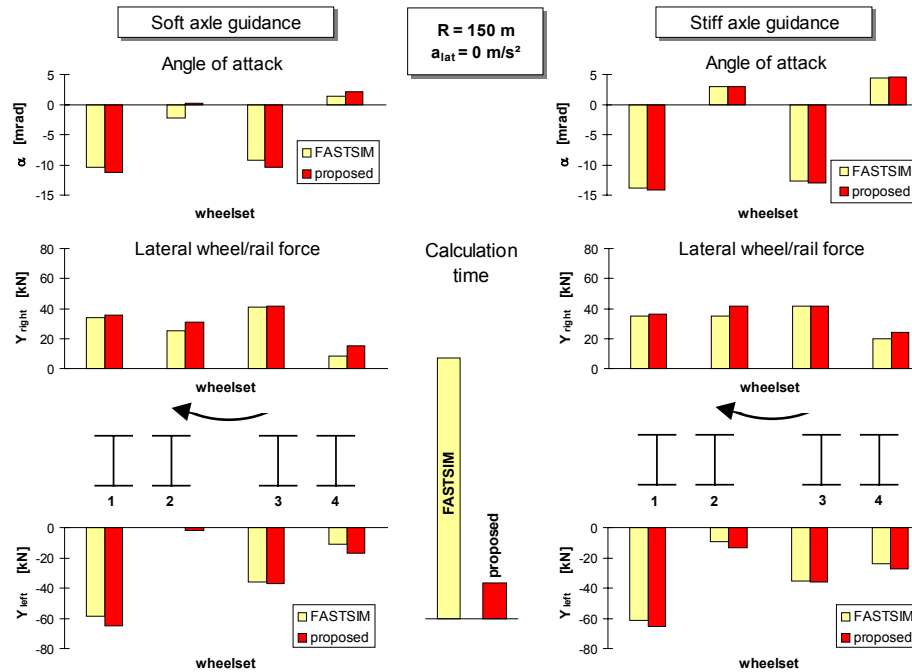


Fig. 6. Comparison of curving simulation results using FASTSIM and the proposed method (simulation package ADAMS/Rail)

4. EXPERIENCE WITH USE OF PROPOSED METHOD

The algorithm has been used in the simulations in different programmes since 1990. In-between, positive experience has been achieved in the research as well as in the industrial application. The algorithm is used in ADAMS/Rail [7] as an alternative parallel to FASTSIM and to the table-book. The calculation time is faster than FASTSIM's and usually faster than the table-book as well and there are no convergence problems during the integration.

To compare the simulation results using the proposed method and FASTSIM, curving analysis have been done with an ADAMS/Rail model of a four-axle locomotive with radial steering wheelsets. The model consists of 51 rigid bodies and possesses 266 degrees of freedom. Fig. 6 shows the lateral forces and angles of attack for two variants of axle guidance stiffness. The results using both methods mentioned are very similar, however there is a big difference in the calculation time. The comparison with measurements in a curve of 300 m radius (Fig. 7) confirms that the results calculated using the proposed method show good agreement. Specially at the leading wheelsets they are nearer to the actually measured values than the results obtained in the simulations using FASTSIM.

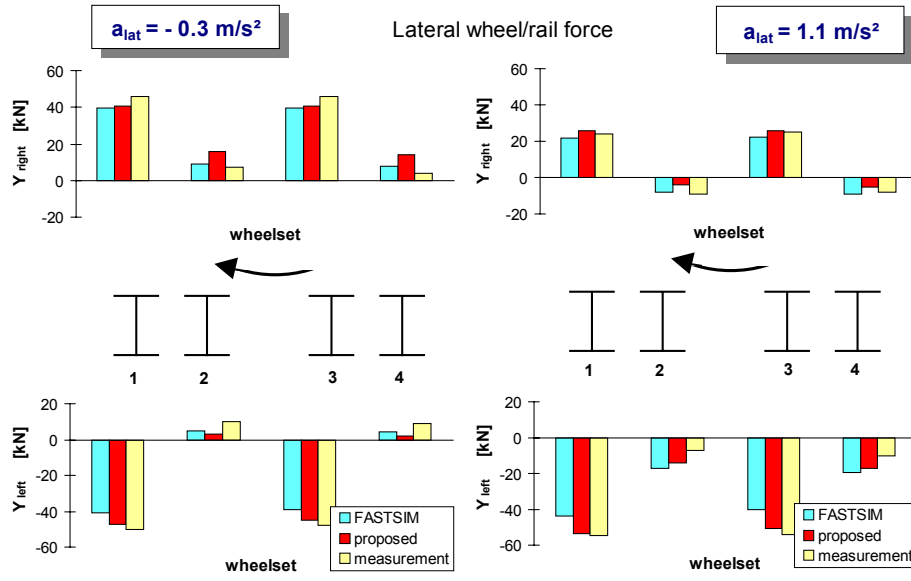


Fig. 7. Measured quasi-static lateral wheel-rail forces of a four axle locomotive in a curve with 300 m radius compared with simulations using the two methods mentioned

5. CONCLUSIONS

The paper discuss a fast method suitable for wheel-rail forces calculation in simulations of rail vehicle behaviour. The method allows calculation of full non-linear forces and takes spin into account. Because of the short calculation time it can be used instead of simple formulae to improve the accuracy or as a substitution of Kalker's method to save computation time. The algorithm has been used in different simulation tools since 1990 with very good experience. The computer code and some test results given in the appendix allows to apply this method in the user's own computer simulation programmes.

REFERENCES

1. Kalker, J. J.: Three-Dimensional Elastic Bodies in Rolling Contact. Kluwer Academic Publishers, Dordrecht, Netherlands 1990
2. Kalker, J. J.: A fast algorithm for the simplified theory of rolling contact. *Vehicle System Dynamics* 11(1982), pp. 1-13
3. Kalker, J. J.: On the rolling contact of two elastic bodies in the presence of dry friction. Thesis, Delft 1967
4. Shen, Z. Y., Hedrick, J. K. and Elkins, J. A.: A comparison of alternative creep force models for rail

- vehicle dynamic analysis. Proc. of 8th IAVSD-Symposium, Cambridge, MA, August 15-19, 1983, pp. 591-605
5. Freibauer, L.: Adheze kola vozidla na dráze. Proc. of "VII. vědecká konference VŠDS, 3. sekce: Dopravní technika - část A", VŠDS Žilina 1983, pp. 214-219. (in Czech)
 6. Polach, O.: Solution of wheel-rail contact forces suitable for calculation of rail vehicle dynamics. Proc. of 2nd Int. Conference on Railway Bogies, Budapest, Sept. 14-16, 1992, pp. 10-17
 7. N.N.: Introducing ADAMS/Rail 9.0, ADAMS/Rail News & Views, No.1, MDI Marburg, Germany, March 1998

APPENDIX – COMPUTER CODE ADH

Used variables :

- FX - longitudinal force in wheel-rail contact F_x
- FY - lateral force in wheel-rail contact F_y
- SX - longitudinal creep s_x
- SY - lateral creep s_y
- OM - spin ψ
- Q - wheel load Q
- F - coefficient of friction f
- A - semiaxis a of the contact ellipse (in longitudinal direction)
- B - semiaxis b of the contact ellipse (in lateral direction)
- G - modulus of rigidity G
- PI - $\pi = 3,14\dots$
- C1 - Kalker's constant c_{11}
- C2 - Kalker's constant c_{22}
- C3 - Kalker's constant c_{23}

Computer code in FORTRAN:

```

SUBROUTINE ADH(Q, F, A, B, SX, SY, OM, C1, C2, C3, FX, FY)
  REAL MI
  REAL KS
  G=8.4E+10
  PI=3.14159
  FX=0
  FY=0
  MI=0
  SYC=SY
  IF (ABS(SY+OM*A).LE.ABS(SYC)) GOTO 10
  SYC=SY+OM*A
10  CONTINUE
  SC=(SX*SX+SYC*SYC)**.5
  IF (SC.EQ.0) GOTO 999
  S=(SX*SX+SY*SY)**.5
  IF (S.EQ.0) GOTO 20
  CJ=((C1*SX/S)**2+(C2*SY/S)**2)**.5
  EP=PI*G*A*B*CJ*SC/(4.*Q*F)
  MI=(EP/(1.+EP*EP)+ATAN(EP))*2.*F/PI
20  KS=1.+6.3*(1.-EXP(-A/B))
  EPM=8.*B*((A*B)**.5)*G*C3*ABS(SYC)/(3.*KS*Q*F)
  DE=((EPM)**2-1.)/((EPM)**2+1.)
  FYS=9.*A*F*KS*(EPM*(-DE**3/3.+DE**2/2.-1./6.))

```

```

/      +1./3.*(1.-DE**2)**(1.5))/16.
FX=-Q*MI*SX/SC
FY=-Q*(MI*SY+FYS*OM)/SC
999  CONTINUE
      PRINT FX, FY
      RETURN
      END

```

Examples of results :

$NY = 0.25$, $G = 8.4 \times 10^{10} \text{ Nm}^{-2}$, $PI = 3.14159$, $Q = 1 \times 10^5 \text{ N}$, $F = 0.3$

$A = 6 \times 10^{-3} \text{ m}$, $B = 6 \times 10^{-3} \text{ m}$, $C1 = 4.12$, $C2 = 3.67$, $C3 = 1.47$:

SX = 0.004 SY = 0 OM = 0 m ⁻¹ FX = -26 732 N FY = 0 N	SX = 0 SY = 0.004 OM = 0 m ⁻¹ FX = 0 N FY = -25 872 N	SX = 0 SY = 0 OM = 0.004 m ⁻¹ FX = 0 N FY = -107 N
SX = 0.002 SY = 0.002 OM = 0.002 m ⁻¹ FX = -16 362 N FY = -16 398 N	SX = 0.004 SY = 0.006 OM = 0 m ⁻¹ FX = -16 098 N FY = -24 147 N	SX = 0.00005 SY = 0.004 OM = 0.008 m ⁻¹ FX = -321 N FY = -25 834 N
SX = -0.00005 SY = 0.004 OM = 0.008 m ⁻¹ FX = 321 N FY = -25 834 N	SX = -0.00005 SY = -0.004 OM = 0.8 m ⁻¹ FX = 323 N FY = 8 259 N	SX = 0.00005 SY = -0.004 OM = -0.008 m ⁻¹ FX = -321 N FY = 25 834 N

$A = 7.5 \times 10^{-3} \text{ m}$, $B = 1.5 \times 10^{-3} \text{ m}$, $C1 = 7.78$, $C2 = 8.14$, $C3 = 6.63$:

SX = 0.002 SY = 0.002 OM = 0 m ⁻¹ FX = -12 606 N FY = -12 606 N	SX = 0 SY = 0.002 OM = 0.002 m ⁻¹ FX = 0 N FY = -13 954 N	SX = 0.002 SY = 0 OM = 0.002 m ⁻¹ FX = -13 421 N FY = -0.3 N
--	--	---

$A = 1.5 \times 10^{-3} \text{ m}$, $B = 7.5 \times 10^{-3} \text{ m}$, $C1 = 3.37$, $C2 = 2.63$, $C3 = 0.603$:

SX = 0.002 SY = 0.002 OM = 0 m ⁻¹ FX = -5 549 N FY = -5 549 N	SX = 0 SY = 0.002 OM = 0.002 m ⁻¹ FX = 0 N FY = -4 919 N	SX = 0.002 SY = 0 OM = 0.002 m ⁻¹ FX = -6 254 N FY = 0 N
--	---	---